JOURNAL OF SOLID STATE CHEMISTRY 80, 56–67 (1989)

New Zirconium Chloride Cluster Phases with the Stoichiometries $Zr_6Cl_{12}Z$ and $Zr_6Cl_{14}Z$ That Are Stabilized by Interstitial Atoms (Z = H, Be, B, C)

ROBIN P. ZIEBARTH AND JOHN D. CORBETT*

Department of Chemistry, Iowa State University, Ames, Iowa 50011

Received November 21, 1988; in revised form February 3, 1989

The syntheses of the following compounds from Zr, ZrX_4, the interstitial Z = H, Be, B, or C, and $M'Cl$ (where appropriate) are reported together with their respective lattice constants: $Zr_6X_{12}H$ (X = Cl or Br), $Zr_6Cl_{12}Be$, $Zr_6Br_{12}B$, $Cs_2ZrCl_6 \cdot Zr_6Cl_{12}Z$ (Z = H or Be), $Zr_6X_{14}C$ (X = Cl or Br), $Zr_6Cl_{14}B$, $MZr_6Cl_{14}Z$ (M = Li–Cs or Tl), and $CsZr_6Br_{14}C$. A number of attempted syntheses of $MZr_6Cl_{14}Z$ phases in which other Z elements could not be encapsulated are also listed. Single-crystal X-ray diffraction data for $Zr_6Cl_{14}C$ and $Zr_6Cl_{14}B$ were also collected and refined (*Cmca*, Z = 4, Nb_6Cl_{14} structure, a = 14.091 (8), 14.243 (1) Å, b = 12.595 (5), 12.640 (2) Å, c = 11.506 (5), 11.546 (1) Å, R = 4.5, 6.1%, respectively). Both the oversized cavity available for the hydride interstitial and the consequences of a matrix effect on dimensions and stability of $Zr_6X_{14}C$ structures when X is changed from chlorine to iodine are discussed.

Introduction

The chemistry of M_6X_{12}-type clusters of the earlier transition element halides that was first revealed in the classic studies of Nb_6Cl_{14}, Ta_6Cl_{15}, Nb_6F_{15}, and the like (*1–4*) has recently been extended to include a large variety of phases containing discrete zirconium (*5–12*) and rare-earth metal (*13–16*) clusters. These discoveries have been accomplished through the agency of an interstitial atom Z bonded within each cluster. These serve to stabilize the new clusters via both the additional electrons contributed to the framework and the strong bonds they form with the metals of the host cluster.

Among the zirconium clusters, the iodides have shown the greater ability to accommodate a variety of Z elements (C, Si, Al, P, Fe, etc.), while the chlorides, in contrast, show the greater structural variety. The latter arises from a characteristic of all M_6X_{12}-type units, the evident presence of a set of good bonding orbitals directed radially (exo) from the vertices of the M_6 core that are always occupied in some manner by another halogen atom (or other base). This feature together with the smaller size of chloride provide a means for the development of a diverse structural series of the type $M^I_x(Zr_6Cl_{12}Z)Cl_n$, wherein additional halide atoms $0 \le n \le 6$ bonded at these vertices determine the character of the overall structural framework. This fairly rigid network (for $n < 6$) may then accommodate (to date) $0 \le x \le 6$ alkali–metal

* To whom correspondence should be addressed.

0022-4596/89 $3.00

cations. The two variables n and x coupled with changes possible in the electronic nature of Z provide a considerable number of compositions in which the clusters can achieve an electron count close to the optimal 14 (*5*). The present article describes our results for $n = 0$ and 2, that is, for cluster compositions $Zr_6Cl_{12}Z$ and $Zr_6Cl_{14}Z$.

Although the composition Zr_6Cl_{12} has been known for some time, questions concerning its actual composition and stability as an empty cluster have remained. The compound was initially obtained in small amounts following $ZrCl/ZrCl_4$ equilibrations near the composition $ZrCl_2$ (*17*). The structure deduced by X-ray powder diffraction was identical to that of "Zr_6I_{12}," which is now known to actually be $Zr_6I_{12}C$ (*5*). However, a consistent preparation of Zr_6Cl_{12} could not be achieved at that time, and sufficient quantities for physical property measurements were not obtained. Subsequently, Imoto *et al.* (*18*) serendipitously obtained Zr_6Cl_{12}, Zr_6Br_{12}, and the related $M_2ZrCl_6 \cdot Zr_6Cl_{12}$ (= $M_2Zr_7Cl_{18}$, M = Na, K, Cs) double salt by thermal decomposition of the corresponding ZrX in the presence of H_2 and, where appropriate, MCl near 750°C. Good yields of the cluster phases were obtained, but these were contaminated by sizable amounts of inseparable ZrH_{2-x}, the formation of which was considered to be the principal driving force for this group of reactions. The greatly improved yields of Zr_6Cl_{12} that were achieved in the presence of hydrogen and the fact that the lattice parameters obtained therefore were 0.3% larger than those for the cluster phase formed in the earlier $ZrCl/ZrCl_4$ equilibrations (*17*) led to speculation that Zr_6Cl_{12} might exist both as an empty cluster and as a hydride, similar to Nb_6I_{11} and $Nb_6I_{11}H$ (*19*). A small nonstoichiometry $Zr_{6+x}Cl_{12}$ was also considered since the end member ($x = 1$) would have what is now known as the closely related $Sc(Sc_6Cl_{12}N)$ structure (*15*) although compositions with intermediate x values have never been found.

Such circumstantial evidence clearly points toward the presence of bound hydrogen in these compounds. This suspicion is augmented by a great deal of subsequent experience demonstrating that a large number of other zirconium and scandium chloride cluster phases can be obtained only when an interstitial element from the second (or other) period is bound within each cluster. A recent NMR study (*20*) has in fact established that the hydrogen in $Zr_6Cl_{12}H$ prepared as described herein is bound within a paramagnetic cluster in which it undergoes rapid motion. Synthetic aspects of this and other systems involving $Zr_6Cl_{12}Z$ clusters are reported in this article.

The diverse interstitial chemistry developed over the past several years for the zirconium iodides pertains principally to the $(M)Zr_6I_{14}Z$ phases with a modified Nb_6Cl_{14} structure, the latter exhibiting a structural matrix that can readily accommodate larger alkali metal cations as well. The success of these investigations among iodides (*5*, *6*, *12*) led us to the present exploration of analogous zirconium chloride systems, studies that have in fact identified some significant differences between the cluster chemistries of the two halides. Research on the chloride system not only provided a number of new $M^IZr_6Cl_{14}Z$ compounds but also led to the discovery of compounds in several new structure types with stoichiometries other than Zr_6Cl_{14} (*7–11*).

Experimental Procedures

Materials

The preparations of $ZrCl_4$, ZrNCl, $ZrH_{1.8}$, and powdered metal; the purification of the alkali metal chlorides; the sources of carbon and boron; the reaction techniques that utilize tantalum containers; and the Guinier powder pattern diffraction

and calculation methods have all been described before (*8*). Beryllium flakes from Pechiney (France) were used as received.

The $ZrBr_4$ reactant was prepared in a similar manner using reactor-grade metal and high-purity Br_2 (<0.02% Cl, A. D. Mackay). The latter was maintained slightly above room temperature during the reaction by placing the arm of the glass apparatus in a bath of warm water while the reaction was initiated by heating the metal in another arm. Multiple vacuum sublimations over zirconium metal and through a frit were again used to purify the material.

Synthetic Techniques

In general, the success of syntheses of cluster-containing phases with identifiable interstitial elements, particularly in cases where the latter is a light element such as H, Be–N, is based largely on the knowledge of what went into a reaction and the relative yields of the product phases obtained rather than on an analysis of the product. Extensive experience has shown that substantially all interstitially stabilized cluster compounds can be prepared in at least 90–95% yields when the appropriate interstitial element is included in the reaction. On the other hand, reactions run in the absence of a workable interstitial produce only simple binary phases like ZrCl, $ZrCl_2$, and $ZrCl_3$ plus $M^{I}_{2}ZrCl_6$ when appropriate and, on occasion, perhaps 5% of a cluster phase that arises from an adventitious impurity, carbon most often.

Syntheses

$Zr_6Cl_{12}H$. This phase was initially prepared directly as a black, microcrystalline material by heating the layered $ZrCl_2$ (3*R*-MoS_2 structure) (*21*) sealed within a Ta tube at 710°C with a large excess of hydrogen at one atmosphere within the outer SiO_2 jacket. The reaction, which was air-quenched after 7 days, produced $Zr_6Cl_{12}H$ in an estimated yield of 60–70%. The other products, a mixture of $ZrCl_4$ and ZrH_{2-x}, attested to the limited stability of the cluster phase with excess hydrogen and to the large equilibrium pressure of $ZrCl_4$ that is generated by disproportionation of the cluster hydride at this temperature.

Improved yields and the elimination of the need for a prior $ZrCl_2$ preparation were accomplished through reactions of stoichiometric amounts of Zr powder, $ZrCl_4$, and $ZrH_{1.8}$ at 700–750°C. These reactions produced $Zr_6Cl_{12}H$ in 70–80% yields after 10–14 days. The remainder was a mixture of $ZrCl_4$ and a phase with the ZrCl structure that had slightly expanded lattice parameters (below). The controlled amounts of hydrogen used in these reactions were critical in the elimination of the ZrH_{2-x} product encountered earlier.

The use of a $ZrCl_4$ excess equivalent to approximately five atmospheres at 700°C plus a two- to fourfold excess of hydrogen pushed the yields of $Zr_6Cl_{12}H$ into the 80–90% range. Subsequent removal of the excess $ZrCl_4$ by sublimation in a static vacuum at 250°C left $Zr_6Cl_{12}H$ and the second phase, which was identified as $ZrClO_xH_y$ ($0 < x < 0.43$, $x + y < 1$) in a ZrCl-type structure based on the powder pattern positions and intensities, its lattice parameters, and a detailed analysis of the hydrogen NMR spectra (*20*). This $ZrClO_xH_y$ phase, which presumably arose from accidental contamination by oxygen, is formed by random insertion of hydrogen and oxygen into tetrahedral metal interstices in the 3*R*-ZrCl structure (*22, 23*).

An attempt to remove the hydrogen from $Zr_6Cl_{12}H$ by heating the material in a sealed Ta tube at 500°C under a dynamic high vacuum for 5 hr resulted in decomposition of the clusters to $ZrCl_2$ plus small amounts of ZrCl and $ZrCl_4$.

A compound containing the same cluster unit in the $K_2ZrCl_6 \cdot Zr_6Cl_{12}H$ structure (*18*) can be obtained in a manner similar to that described above for $Zr_6Cl_{12}H$ by the

inclusion of a stoichiometric amount of the appropriate CsCl or KCl in the reaction. Significantly lower autogenous $ZrCl_4$ pressures are encountered over these phases, and a two-atmosphere equivalent of excess $ZrCl_4$ provides a yield of about 90%. A mixture of $ZrClO_xH_y$ and $M^I_2ZrCl_6$ make up the remainder of the product. In contrast to $Zr_6Cl_{12}H$, where only microcrystalline materials are obtained, reactions producing $M^I_2Zr_7Cl_{18}H$ often provide moderate-sized, well-formed, dark red crystals. These products were not studied further.

Both $Zr_6Cl_{12}H$ and the related $M_2Zr_7Cl_{18}H$ compounds contain 13-electron clusters. The 14-electron analogs $Zr_6Cl_{12}Be$ and $Cs_2Zr_7Cl_{18}Be$ were prepared in 95 + % yields (i.e., single phase to Guinier powder diffraction) through reactions of stoichiometric amounts of Zr powder, $ZrCl_4$, Be flakes, and, if appropriate, CsCl at 800°C for 14 days. Crystal growth of the red-brown compounds was negligible. The phase $Cs_2Zr_7Cl_{18}Be$ was initially synthesized in about 50% yield in a reaction stoichiometrically loaded to produce $CsZr_6Cl_{14}Be$ (below). Interestingly, the potassium double salt $K_2Zr_7Cl_{18}Be$ was not obtained under these conditions, in contrast to the behavior of the hydride; rather, reactions loaded with the stoichiometric proportions yielded a mixture of $KZr_6Cl_{13}Be$ (*24*) and K_2ZrCl_6. Although their syntheses have not been attempted, $M_2Zr_7Cl_{18}Be$ compounds with M = Na–Cs can probably be produced at lower temperatures by the direct reaction of $Zr_6Cl_{12}Be$ with M_2ZrCl_6 in a $ZrCl_4/MCl$ melt.

$Zr_6Cl_{14}C$. The compound was initially obtained as the major product (95 + %) from an 850°C reaction designed to prepare "$Zr_6Cl_{15}C$" (*9*) starting with stoichiometric amounts of Zr powder, $ZrCl_4$, and C in the form of graphite. The dark red-brown material was unambiguously identified as $Zr_6Cl_{14}C$ by the synthesis plus a comparison of the observed powder diffraction pattern with that calculated with the aid of the published parameters for Nb_6Cl_{14} (*2*). The excess $ZrCl_4$ present in the reaction appears to be approximately the amount necessary to generate the equilibrium $ZrCl_4$ pressure over the product at 850°C and therefore to repress its extensive decomposition. The $ZrCl_4$ excess could again be easily removed by sublimation under static vacuum at ~250°C. A variety of temperatures from 700 to 950°C were used to prepare $Zr_6Cl_{14}C$, but crystal growth was negligible in all cases. Attempts to improve crystal growth by a variety of other techniques, including the use of $M^ICl/ZrCl_4$ fluxes, temperature gradients, mobile carbon sources such as paraffin, and slow cooling were also tried but with minimal success.

Macrocrystals of $Zr_6Cl_{14}C$ were obtained on two occasions, however, both in reactions contaminated with oxygen. The crystal used for the single-crystal diffraction study (below) came from a reaction designed to prepare "$Na_4Zr_6Cl_{18}H$" under H_2 at 700°C. A leak in the hydrogenation system during the reaction surrounded the tantalum reaction tube with a hydrogen/air mixture. The carbon source in the reaction is unknown. A Guinier powder diffraction pattern of the ground crystals showed the lattice parameters to be slightly larger than those obtained for $Zr_6Cl_{14}C$ prepared with graphite (above). A later reaction, loaded stoichiometrically to prepare $NaZr_6Cl_{15}{}^{13}C$ (*9*), produced gem-like crystals of $Zr_6Cl_{14}C$ instead, but the large amounts of $ZrClO_x$ (*22*) also present indicated the reaction had become contaminated with oxygen, presumably from an impure ^{13}C source. Lattice parameters in this case showed no significant deviation from those obtained from $Zr_6Cl_{14}C$ prepared with graphite. Restudy of the structure with these better crystals was not deemed worthwhile.

Reasons for the difficulties encountered in growing these crystals are not clear, particularly in light of the results with many

zirconium iodide carbide cluster phases where crystal growth is exceptional (*5, 6*). The experiences with the reactions contaminated with oxygen, however, suggest that chemical transport of carbon by CO (*25*) may be useful for crystal preparation provided sufficient pressures can be maintained in the presence of the reactants and the container. Additional work will be required to verify the transport reaction.

The new $Zr_6Cl_{14}B$ was repeatedly synthesized in 5–10% yields in 950°C reactions stoichiometrically proportioned to yield Zr_2Cl_2B (*26*). The highly reflective, black, gem-like crystals were easily separated from the dark brown, microcrystalline Zr_2Cl_2B. The crystals were often twinned and mixed with similarly shaped crystals of $Zr_6Cl_{13}B$ (*24*). Although prepared only in low yield, the Guinier lattice parameters clearly support the identification of the material as $Zr_6Cl_{14}B$ rather than the corresponding carbide that might have formed from adventitious carbon. The identification is further supported by a single-crystal X-ray diffraction study (below). Reactions of Zr powder, $ZrCl_4$, and amorphous B powder in amounts suitable for the preparation of the 13-electron $Zr_6Cl_{14}B$ invariably produced 14-electron $Zr_6Cl_{13}B$ (and $ZrCl_4$) instead and in greater than 95% yield. Single-phase amounts of $Zr_6Cl_{14}B$ large enough for physical property measurements were not obtained, even with more $ZrCl_4$ present.

The 14-electron $M^IZr_6Cl_{14}B$ phases (M = Li–Cs, Tl) in the Nb_6Cl_{14} (or $CsZr_6I_{14}C$ (*5*)) host structure were obtained in 95+% yields after reaction at 850°C for 10–21 days of stoichiometric amounts of Zr powder, $ZrCl_4$, amorphous B powder, and M^ICl, except for $TlZr_6Cl_{14}B$ where Tl metal was used. Good crystal growth was obtained with M^I = Na, K, Rb, and Cs.

The syntheses of a variety of other $M^IZr_6Cl_{14}Z$ phases containing third-period interstitial elements or with cluster electron counts of 13 to 16 were attempted but without success. Several new compounds were obtained, but with stoichiometries other than $M^IZr_6Cl_{14}Z$. A compilation of the compounds sought, the reaction temperatures, and the major products found in these explorations is given in Table I. Although the size of the interstitial atom appears to be an important factor in the failure to obtain other $M^IZr_6Cl_{14}Z$ compounds with Z = Al, Si, the recent syntheses of $CsZr_6Cl_{15}Fe$ and $Zr_6Cl_{15}Co$ (*27*), both with comparatively large interstitial atoms, suggest that other factors are also important. The thermodynamic stability of alternate phases is clearly the overriding criterion.

Structural Refinements

Two octants of data were collected at room temperature with the aid of monochromatic Mo$K\alpha$ radiation and a Syntex $P2_1$ diffractometer from the small, gem-like crystals of "$Zr_6Cl_{14}C$" and $Zr_6Cl_{14}B$ described above. Absorption corrections were made on the basis of one and two ψ

TABLE I

UNSUCCESSFUL REACTIONS WITH $M^IZr_6Cl_{14}Z$ TARGETS[a]

Target compound	Cluster electron count	Reaction temperature (°C)	Major products
$Zr_6Cl_{14}Si$	14	800	Zr_5Si_3, $ZrCl_4$ $ZrCl$, $ZrCl_{3-x}$
$CsZr_6Cl_{14}Al$	14	800	Unidentified multiphase products
$CsZr_6Cl_{14}Be$	13	800	$Cs_2Zr_7Cl_{18}Be$
$BaZr_6Cl_{14}Be$	14	800	Unidentified
$Zr_6Cl_{14}B$	13	850	$Zr_6Cl_{13}B$
$HgZr_6Cl_{14}B$	15	850	Hg, $Zr_6Cl_{13}B$
$CsZr_6Cl_{14}C$	15	850	$CsZr_6Cl_{15}C$[b]
$KZr_6Cl_{14}C$	15	850	$KZr_6Cl_{15}C$[b]
$NaZr_6Cl_{14}C$	15	850	$Na_{0.5}Zr_6Cl_{15}C$[c]
$Zr_6Cl_{14}N$[d]	15	850	1*T*-Zr_2Cl_2N, 3*R*-Zr ClN_x,[e] ZrN, $ZrCl_4$
$Zr_6Cl_{14}O$[f]	16	850	$ZrClO_x$, $ZrCl_{3-x}$

[a] Stoichiometric proportions of the reactants were used.
[b] Ref. (*8*).
[c] Ref. (*9*).
[d] ZrNCl was the nitrogen source.
[e] Ref. (*26*).
[f] ZrO_2 was the oxygen source.

TABLE II

SUMMARY OF CRYSTALLOGRAPHIC AND REFINEMENT DATA FOR $Zr_6Cl_{14}C$ AND $Zr_6Cl_{14}B$

	$Zr_6Cl_{14}C$	$Zr_6Cl_{14}B$
Space group	*Cmca*	*Cmca*
Z	4	4
a (Å)	14.091(8)	14.243(1)[a]
b	12.595(5)	12.640(2)
c	11.506(5)	11.546(1)
V (Å^3)	2042(2)	2078.6(5)
Crystal dimen. (mm)	0.15 × 0.15 × 0.20	0.15 × 0.15 × 0.15
Radiation	Mo$K\alpha$, graphite monochromater	Mo$K\alpha$, Zr β-filter
2θ (max) (deg)	55.0	55.0
Scan mode	ω	$2\theta/\theta$
Reflections		
Octants meas.	$h, k, \pm l$	h, k, l
Checked	2391	1252
Obs[b]	1653	652
Indep. refl.	894	652
R(ave) (%)	1.8	—
μ (cm^{-1})	46.7	45.9
Transm. coeff. range, normalized	0.76–1.00	0.82–1.00
R^c (%)	4.5	6.1
$R_w{}^d$ (%)	7.9	7.9

[a] Lattice parameters from Guinier powder diffraction with Si as an internal standard.

[b] $F_o \geq 3\sigma_F$ and $I_o > 3\sigma_I$.

[c] $R = \Sigma(|F_o| - |F_c|)/\Sigma|F_o|$.

[d] $R_w = [\Sigma w(|F_o| - |F_c|)^2/\Sigma w|F_o|^2]^{1/2}$, $w = \sigma_F^{-2}$.

scans, respectively. Details of the data collections are given in Table II.

Refinement of the known structure type began with the niobium and chlorine positional parameters from Nb_6Cl_{14} (*2*) after the appropriate transformation from the nonstandard space group *Bbam* to *Cmca*. The zirconium and chlorine positions and isotropic thermal parameters refined uneventfully to $R = 7.3\%$, at which point a Fourier map showed an approximately seven-electron residual in the cluster center. Because of the unknown nature of the interstitial atom, several refinements were carried out with different elements in the interstitial site. Carbon was finally chosen as the interstitial atom because of both the similarity of the single crystal's lattice constants to more precise Guinier values for $Zr_6Cl_{14}C$ prepared from graphite (below) and the good consistency of the refined Zr–Zr and Zr–C distances with those in other structurally characterized, 14-electron, carbon-centered zirconium chloride clusters (*8, 28*). The transferability of these distances between different phases is generally very good. Boron and nitrogen were systematically eliminated because $NaZr_6Cl_{14}B$ and $Zr_6Cl_{15}N$, respectively, were known to form under the conditions used with purposeful addition of those interstitial elements (above). In addition, $Zr_6Cl_{14}B$ shows significantly different lattice parameters (Table II). Sodium and oxygen interstitial atoms were ruled out because the compounds could not be independently prepared with the appropriate elements present.

The structural refinement with carbon converged at $R = 4.5\%$ and $R_w = 7.9\%$. (Experience suggests the latter is high because errors assigned to weak reflections are too small (*15*).) The refined carbon occupancy, 1.4 (1) with $B = 0.4$ (3) Å^2 (possibly correlated), was not very well determined, but this and the slightly expanded lattice parameters over those of $Zr_6Cl_{14}C$ suggest that a "mixed interstitial," primarily carbon in character, may be present. Possibly combinations of interstitial atoms and the stabilities of the compounds formed are presently unknown. Evidence for mixed interstitials in other cluster systems that originated with adventitious sources is fairly conclusive, however (*5, 6, 15, 26, 29*).

Refinement of the structure of $Zr_6Cl_{14}B$ was carried out starting with the atomic positions of zirconium and chlorine from $Zr_6Cl_{14}C$. A Fourier map calculated after isotropic refinement of the zirconium and chlorine parameters showed a five-electron residual in the cluster center, and this was included as a boron atom in subsequent calculations. The model converged to residuals of $R = 6.1\%$, and $R_w = 7.9\%$ after anisotropic refinement of the zirconium and chlorine thermal parameters and a reweighting of the data set in overlapping

group sorted by F_o to correct for underestimated errors for the weaker reflections. The interstitial B refined to an occupancy of 1.0 (1) with B = 2 (1) Å^2. The final difference map showed several 0.5–1.0/electron Å^3 features, all of which were associated with refined atom positions. The potential cation site at (0, 0, 0) (*5*) was unoccupied. The thermal ellipsoids were relatively small ($0.8 \leq B_{iso} \leq 1.4$), but these showed a slight elongation in the **b** direction, presumably a consequence of poor crystal quality, an inadequate absorption correction, or both.

Positional parameters for $Zr_6Cl_{14}C$ and $Zr_6Cl_{14}B$ are listed in Table III. Listings of the observed and calculated structure factor amplitudes and the anisotropic thermal parameters for both structures are available from an author (J.D.C.) on request. Programs for data reduction, absorption correction, least-squares refinement, and mapping have been referenced before, as have the sources of the neutral atom scattering factors which included corrections of the real and imaginary contributions to anomalous dispersion (*30*).

TABLE III

POSITIONAL PARAMETERS FOR $Zr_6Cl_{14}C$ AND $Zr_6Cl_{14}B$

Atom	x	y	z	B_{iso} (Å^2)
		$Zr_6Cl_{14}C$		
Zr1	0.38286(8)	0.07095(9)	0.8826(1)	0.91(4)
Zr2	0	0.3507(1)	0.8926(1)	0.93(6)
Cl1	0.1242(2)	0.0876(2)	0.2497(3)	1.5(1)
Cl2	0.1240(2)	0.2551(2)	0.0083(3)	1.3(1)
Cl3	¼	0.3448(4)	¼	1.4(2)
Cl4	0	0.1582(4)	0.7629(4)	1.4(2)
Cl5	0.2474(3)	0	0	1.3(1)
C[a]	0	0	½	0.4(3)
		$Zr_6Cl_{14}B$		
Zr1	0.3844(1)	0.0715(1)	0.8827(1)	0.82(5)
Zr2	0	0.3502(2)	0.8905(2)	0.83(8)
Cl1	0.1240(3)	0.0881(3)	0.2486(4)	1.2(2)
Cl2	0.1252(3)	0.2547(3)	0.0069(4)	1.2(1)
Cl3	¼	0.3431(5)	¼	1.4(2)
Cl4	0	0.1592(4)	0.7623(5)	1.1(2)
Cl5	0.2491(4)	0	0	1.3(2)
B[b]	0	0	½	2(1)

[a] Occupancy refined to 1.4 (1).
[b] Occupancy refined to 1.0 (1).

TABLE IV

CELL PARAMETERS (Å) AND VOLUMES (Å^3) OF $Zr_6Cl_{12}Z$ AND $Cs_2Zr_7Cl_{18}Z$

Compound	a	c	V	Cluster electron count
$Zr_6Cl_{12}H$[b]	13.005(1)	8.808(1)	1290.2(3)	13
$Zr_6Cl_{12}H$[c]	13.0071(8)	8.808(1)	1290.5(2)	13
$Zr_6Cl_{12}H$[d]	12.983(1)	8.792(2)	1283.4(4)	13
$Zr_6Cl_{12}H$[e]	12.975(1)	8.794(2)	1282.1(4)	13
$Zr_6Cl_{12}H$[e]	12.9854(7)	8.790(1)	1283.5(2)	13
$Zr_6Cl_{12}Be$	13.1608(8)	8.840(1)	1324.6(2)	14
$Zr_6Br_{12}B$	13.633(1)	9.307(1)	1498.0(3)	15
$Cs_2ZrCl_6 \cdot Zr_6Cl_{12}H$[b]	9.595(1)	26.186(8)	2089.0(1)	13
$Cs_2ZrCl_6 \cdot Zr_6Cl_{12}Be$	9.6461(9)	26.404(3)	2125.4(5)	14

[a] All cell values were obtained from Guinier powder diffraction data at room temperature, space group $R\bar{3}$, λ = 1.54056 Å.
[b] Ref. (*18*); preparation from ZrCl and H_2 (+ CsCl); product contains ZrH_{2-x}.
[c] This work; preparation from $ZrCl_2$ and H_2; product contains ZrH_{2-x}.
[d] Ref. (*17*); from ZrCl, $ZrCl_3$, and adventitious hydrogen.
[e] This work; preparation from Zr, $ZrCl_4$, and $ZrH_{1.8}$.

Results and Discussion

$Zr_6Cl_{12}Z$ Compounds

The new Zr_6Cl_{12} cluster compounds, their lattice parameters determined by Guinier powder diffraction, and the cluster-based electron counts therefore are listed in Table IV. Discussion of these examples requires an understanding of the structure ($Zr_6I_{12}C$ type, space group $R\bar{3}$ (*5*, *29*)), which is shown in Fig. 1 in the [110] projection. The principal building block of the structure is the Zr_6Cl_{12} cluster, a trigonal antiprismatic Zr_6 core that is surrounded by 12 chlorine atoms bridging all edges of the metal cluster. As seen in the figure, a cubic-close-packed array of these Zr_6Cl_{12} clusters is arranged with the $\bar{3}$ axis of each normal to the layer direction and parallel to **c**. An exten-

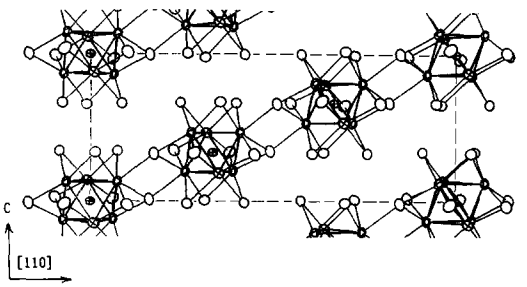

FIG. 1. A [110] projection of the rhombohedral structure of $Zr_6Cl_{12}H$ (*18, 20*). The *c* axis runs vertically in the plane of the figure, perpendicular to the close-packed layers. A hydrogen atom occupies the center of each Zr_6Cl_{12} cluster.

sive sharing of the chlorine atoms between clusters is necessitated by the stoichiometry and the terminal bonding requirements of the six metal atoms in each cluster. Specifically, the six chlorine atoms around the waist, i.e., those bridging metal cluster edges that have a component parallel to the $\bar{3}$ axis, serve as more distant terminal chlorine atoms to metal vertices on six adjacent clusters, three above and three below. The connectivity is conveniently formulated as $[Zr_6Cl_6^iCl_{6/2}^{i-a}]Cl_{6/2}^{a-i}$, where Cl^{i-a} and Cl^{a-i} reflect the connectivity just described while Cl^i is not shared. Hydrogen or beryllium appears to be essential to the formation of the listed phases, at least for samples prepared under equilibrium, high-temperature conditions. The presence of a hydrogen atom within each cluster in $Zr_6Cl_{12}H$ has been conclusively established by solid-state NMR studies (*20*).

It will be noted that the packing and cluster bridging in this structure creates an empty trigonal antiprismatic chlorine polyhedron site above and below each cluster along the $\bar{3}$ axis (at 0, 0, ½, etc.). The site is completely occupied by a seventh Sc^{3+} cation in the closely related $Sc(Sc_6Cl_{12}N)$-type structure (*15*) that is formed in many rare-earth–metal systems (*16*), but no conclusive evidence for its occupation in any zirconium halide phase has been obtained.

The structure of the double salts $M_2Zr_7Cl_{18}Z$ is built-up of an expanded cubic-close-packed array of $Zr_6Cl_{12}Z$ clusters similar to that in $Zr_6Cl_{12}H$ and in the same space group ($R\bar{3}$). However, chlorine atoms from $ZrCl_6^{2-}$ anions located on the octahedral sites between the clusters now provide all the terminal chlorine atoms for the $Zr_6Cl_{12}H$ clusters.

The cluster dimensions in $Zr_6Cl_{12}H$ should be very similar to those in $K_2Zr_7Cl_{18}H$, in which the Zr–Zr distances are 3.178 (1) and 3.224 (1) Å, while the Zr-cluster center distance is 2.264 (1) Å (*18*). The same cluster dimensions are found in $Li_6Zr_6Cl_{18}H$ as well (*31*). The Zr-centroid distance in these is significantly longer than typical Zr–H distances, 2.08–2.10 Å, which presumably accounts for the "rattling" of hydrogen seen by NMR in $Zr_6Cl_{12}H$ (*20*). The cluster dimensions in this case are therefore determined primarily by Zr–Zr interactions and provide a valuable baseline regarding minimum interstitial size for rigidity. The presence of hydrogen in $Zr_6Cl_{12}H$ undoubtedly extends to the clusters in the other $M_2^IZr_7Cl_{18}(H)$ phases, $Zr_6Br_{12}(H)$ (*18*), and the recently studied $Li_6Zr_6Cl_{18}H$ (*31*).

An unexpected result of this study is the presence of two slightly different sets of lattice parameters for the $Zr_6Cl_{12}H$ such that the volumes of the trigonal cells differ by 7–8 Å^3 (0.6%) (Table IV), thus confirming the earlier results (*18*). Samples prepared by the reaction of ZrCl or $ZrCl_2$ with excess H_2 exhibit the large cell, while $Zr_6Cl_{12}H$ products synthesized by the reaction of $Zr/ZrCl_3$ or $ZrCl/ZrCl_4$ with adventitious or controlled amounts of hydrogen, respectively, exhibit the smaller parameters. The NMR study on the last material and the need for hydrogen in the preparation of the clusters in good yield with either cell volume rules out hydrogen in one cluster and not the

other as the cause. Rather, the difference appears to be closely linked to the degree of reduction of the starting mixture and, therefore, to the presence or absence of ZrH_{2-x} in the product. The larger cell is found only in equilibrium with ZrH_{2-x} derived by disproportionation. A reasonable explanation, previously advanced (*18*), is that a small fractional occupancy of the isolated cation site in $Zr_6Cl_{12}H$ by Zr^{4+} cations is responsible for the larger cell material. Complete occupation of the cation site as known for numerous $M_7X_{12}Z$ compounds would be easily recognized by changes in powder diffraction intensities of certain reflections, but the results of a small fractional occupancy suggested for $Zr_{6+x}Cl_{12}H$ would be virtually indistinguishable from powder data for the stoichiometric compound. The consistency of the two sets of lattice parameters within their respective groups may indicate two discrete compositions or simply a failure thus far to produce intermediate compositions. Although the effects are small, further synthetic work as well as structural studies of both the large and small cell materials may be able to elucidate the factors responsible.

The new phases $Zr_6Cl_{12}Be$ and $Cs_2Zr_7Cl_{18}Be$ were the first two examples of transition metal clusters centered by beryllium atoms. Each is isostructural with the corresponding hydride. The increase of 13–14 Å^3 per cluster observed in both compounds over the corresponding hydrides is a reflection of the inclusion of a significantly larger interstitial atom. Structural characterization by single-crystal X-ray diffraction has not been carried out because of the lack of suitably sized crystals. Meanwhile, other beryllides have been structurally characterized, $KZr_6Cl_{13}Be$ (*7, 24*), $K_3Zr_6Cl_{15}Be$ (*10*), and $Na_4Zr_6Cl_{16}Be$ (*11*).

$Zr_6Cl_{14}Z$ Compounds

The 11 new phases of this stoichiometry that have been prepared in this study are listed in Table V along with their unit cell dimensions. The alkali metal cation present in several $M^IZr_6X_{14}Z$ derivatives is accommodated within a 12-coordinate chlorine polyhedron between the clusters (*5, 29*). The case for $LiZr_6Cl_{14}B$ is perhaps ambiguous, since the differences in lattice constants from those for $Zr_6Cl_{14}B$ are so small; magnetic susceptibility or NMR results will be required to verify lithium incorporation in the same or some other site although the achievement of a 14-e$^-$ cluster and the higher yield in the presence of lithium make its inclusion quite probable. These phases are all isostructural with Nb_6Cl_{14} (*2*), save for Z and M^I, if any, as well as with a variety of zirconium iodide analogs (*5, 6, 12, 32*) which include examples with Z = B, C, Al, Si, P, Ge, Mn, Fe, Co, K, but not H. Attempts to make analogous chlorides centered by the main group elements Si and Al were all unsuccessful (Table I), although it is noteworthy that $Zr_6X_{14}Fe$ has been obtained for X = Cl or Br (*27*).

Single-crystal parameters have been established for $Zr_6Cl_{14}C$ and $Zr_6Cl_{14}B$ (Tables II and III). While these do not represent the best structural refinements available for

TABLE V

CELL PARAMETERS (Å) AND VOLUMES (Å^3) OF $Zr_6Cl_{14}Z$ (Z = C, B) AND $M^IZr_6Cl_{14}B$(M = Li–Cs, Tl) COMPOUNDS AND TWO BROMIDE ANALOGS[a]

Compound	*a*	*b*	*c*	*V*
$Zr_6Cl_{14}C$	14.021(2)	12.562(2)	11.480(3)	2022.0(8)
$Zr_6Cl_{14}C$[b]	14.091(8)	12.595(5)	11.506(5)	2042(2)
$Zr_6Cl_{14}B$	14.243(1)	12.640(2)	11.546(1)	2078.6(5)
$LiZr_6Cl_{14}B$[c]	14.267(3)	12.647(3)	11.536(2)	2081.4(8)
$NaZr_6Cl_{14}B$	14.110(2)	12.655(2)	11.535(2)	2059.6(5)
$KZr_6Cl_{14}B$	14.095(1)	12.640(1)	11.570(1)	2061.2(3)
$RbZr_6Cl_{14}B$	14.113(1)	12.647(2)	11.624(1)	2074.4(4)
$CsZr_6Cl_{14}B$	14.143(1)	12.678(2)	11.707(1)	2098.9(4)
$TlZr_6Cl_{14}B$	14.095(1)	12.621(1)	11.583(1)	2060.6(3)
$Zr_6Br_{14}C$	14.690(3)	13.229(3)	11.991(3)	2330(1)
$CsZr_6Br_{14}$	14.737(1)	13.297(2)	12.108(1)	2372.7(5)

[a] All values were obtained from Guinier powder diffraction data, λ = 1.54056 Å; space group *Cmca*.
[b] Data crystal; diffractometer values.
[c] See text.

M_6X_{14} phases, they are important as the only structurally refined $Zr_6Cl_{12}Z$-type clusters in phases that are isostructural with many $Zr_6I_{12}Z$ examples since the iodides do not (yet) include examples of other chloride stoichiometries, e.g., $Zr_6Cl_{13}Z$, $Zr_6Cl_{15}Z$, etc. (*7–10*). In addition, the $Zr_6Cl_{14}B$ structural results verified the presence of the boron interstitial atom when the phase could only be prepared in the 5–10% yields typically associated with adventitiously stabilized products, in this case evidently because of the high stability of the competing 14-electron cluster phase $Zr_6Cl_{13}B$. Some interatomic distances within $Zr_6Cl_{14}C$ and $Zr_6Cl_{14}B$ are given in the Table VI. The structure is illustrated in Fig. 2 but with only the bridging chlorine atoms about the central cluster included to improve the clarity.

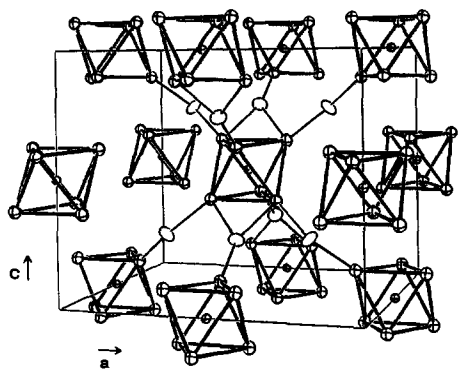

FIG. 2. The structure of $Zr_6Cl_{14}C$ emphasizing the intercluster connectivity. Mirror planes lie at $x = 0$ and $\frac{1}{2}$. Although the Cl^i atoms not involved in intercluster connectivity have been omitted for clarity, the close-packed anion layers stacked in the c direction can easily be imagined between layers of metal atom (90% probability thermal ellipsoids).

TABLE VI

INTERATOMIC DISTANCES IN $Zr_6Cl_{14}C$ AND $Zr_6Cl_{14}B$ (Å)[a]

		$Zr_6Cl_{14}C$	$Zr_6Cl_{14}B$
Zr–Zr			
Zr1–Zr1	(×2)[b]	3.235(2)	3.256(3)
Zr1–Zr1	(×2)	3.290(2)	3.294(3)
Zr1–Zr2	(×4)	3.217(2)	3.247(2)
Zr1–Zr2	(×4)	3.218(2)	3.248(2)
$\bar{d}$		3.232	3.257
Zr–Z			
Zr1–Z	(×4)	2.307(1)	2.316(1)
Zr2–Z	(×2)	2.243(2)	2.277(2)
$\bar{d}$		2.286	2.303
Zr–Cl^i			
Zr1–Cl5	(×2)	2.497(3)	2.523(4)
Zr1–Cl2	(×2)	2.522(3)	2.544(4)
Zr1–Cl1	(×2)	2.512(3)	2.546(4)
Zr2–Cl1	(×2)	2.518(3)	2.532(4)
Zr2–Cl2	(×2)	2.503(3)	2.583(4)
Zr–Cl^{i-a}			
Zr1–Cl4	(×2)	2.591(3)	2.597(4)
Zr–Cl^{a-i}			
Zr2–Cl4	(×2)	2.836(4)	2.832(6)
Zr–Cl^{a-a}			
Zr1–Cl3	(×4)	2.630(2)	2.679(3)

[a] Zr2, Z, and Cl4 lie on the mirror plane perpendicular to **a** (Fig. 1).

[b] Number of times the distance occurs per cluster or cation.

Any attempt at an a priori description of the $Zr_6Cl_{14}Z$ structure would lead to a recognition that the stoichiometry of the compound and the requirement that terminal positions at each metal vertex be occupied necessitate a complicated sharing of chlorine atoms between clusters. These are achieved as follows: Ten of the 12 edge-bridging Cl^i atoms on each cluster are unshared, while the remaining two serve in a dual capacity as Cl^i atoms on one cluster and Cl^a atoms on adjacent clusters. The latter lie on a vertical mirror plane at $x = \frac{1}{2}$ in Fig. 2. The remaining four terminal positions on each cluster are filled by four additional chlorine atoms Cl^{a-a} that serve a similar function in adjacent clusters. The connectivity in $Zr_6Cl_{14}C$ is therefore formulated $[Zr_6Cl^i_{10}Cl^{i-a}_{2/2}]Cl^{a-i}_{2/2}Cl^{a-a}_{4/2}$. The structure can also be described starting with close-packed chlorine atoms (*18, 29*).

Structural trends established by previous

$M^{I}Zr_6I_{14}Z$ studies are found to carry over to the chloride clusters in virtually all respects. The $Zr_6Cl_{12}Z$ clusters in both $Zr_6Cl_{14}C$ and $Zr_6Cl_{14}B$ exhibit the slight tetragonal compression expected on the basis of the effects of the asymmetric bonding of the terminal chlorine atoms, namely longer Zr–Cl^a and shorter opposing Zr–Z distances at those vertices where three coordinate Cl^{a-i} atoms are bound (Fig. 2). The Zr–Zr and Zr–Z distances lengthen, as expected, when going from the carbide to the boride and are consistent both with those calculated from tabulated or derived (from NaCl-type transition metal carbides and borides) crystal radii and with distances from other structurally characterized zirconium chloride clusters (*28*). Distances in the zirconium iodide clusters tend to be slightly larger, presumably because of a matrix effect associated with the larger, more tightly packed iodine atoms, e.g., by 0.08 and 0.05 Å in average Zr–Zr and Zr–C distances in the analogous $Zr_6I_{14}C$ (*5*) relative to those in $Zr_6Cl_{14}C$.

The most significant consequence of the halide size between chloride vs iodide clusters is in the degree to which the zirconium atoms are pulled in from the square faces of the approximate cuboctahedron formed by the X^i atoms because of X^i–X^i repulsion (matrix effect). In $Zr_6I_{14}C$ each zirconium atom is nearly 0.5 Å inside the square face of the I^i atoms that surround it, which compares with the approximately 0.25-Å displacement in $Zr_6Cl_{14}C$ with the smaller halide. This difference plays a significant role in the character of the eighth metal–metal bonding (a_{2u}) orbital, the greater Zr–Cl^i antibonding component thereto then serving to destabilize the 15- and 16-electron chloride clusters relative to the behavior of the iodides (*5, 28*). This serves to make 14-electron clusters relatively more stable for chloride. No $Zr_6Cl_{12}Z$ or $Zr_6Cl_{14}Z$ examples have been obtained with more than 14 electrons per cluster (Tables I, IV, V) although two bromides with 15 have been synthesized, $Zr_6Br_{12}B$ and $CsZr_6Br_{14}C$ (Tables IV, V), consistent with above interpretation. The 16-electron $Zr_6I_{12}C$ appears particularly stable with notably short Zr–C distances, 2.259 Å (*5*) vs 2.339 Å in $Zr_6I_{14}C$ (*6*) and 2.286 Å in $Zr_6Cl_{14}C$.

Acknowledgments

This research was supported by the National Science Foundation, Solid-State Chemistry, via grant DMR-8318616 and was carried out in facilities of the Ames Laboratory, DOE. RPZ was also supported by Departmental Gilman and Procter and Gamble Fellowships.

References

1. H. Schäfer and H.-G. Schnering, *Angew. Chem.* **76,** 833 (1964).
2. A. Simon, H.-G. von Schnering, H. Wöhrle, and H. Schäfer, *Z. Anorg. Allg. Chem.* **339,** 155 (1965).
3. D. Bauer and H.-G. von Schnering, *Z. Anorg. Allg. Chem.* **361,** 259 (1968).
4. H. Schäfer, H.-G. Schnering, K.-J. Niehues, and H. G. Nieder-Vahrenholz, *J. Less-Common Met.* **9,** 95 (1965).
5. J. D. Smith and J. D. Corbett, *J. Amer. Chem. Soc.* **107,** 5704 (1985).
6. J. D. Smith and J. D. Corbett, *J. Amer. Chem. Soc.* **108,** 1927 (1986).
7. R. P. Ziebarth and J. D. Corbett, *J. Amer. Chem. Soc.* **107,** 4571 (1985).
8. R. P. Ziebarth and J. D. Corbett, *J. Amer. Chem. Soc.* **109,** 4844 (1987).
9. R. P. Ziebarth and J. D. Corbett, *J. Less-Common Met.* **137,** 21 (1988).
10. R. P. Ziebarth and J. D. Corbett, *J. Amer. Chem. Soc.* **110,** 1132 (1988).
11. R. P. Ziebarth and J. D. Corbett, *Inorg. Chem.* **28,** 626 (1989).
12. T. Hughbanks, G. Rosenthal, and J. D. Corbett, *J. Amer. Chem. Soc.* **110,** 1511 (1988).
13. E. Warkentin, R. Masse, and A. Simon, *Z. Anorg. Allg. Chem.* **491,** 323 (1982).
14. A. Simon, *J. Solid State Chem.* **57,** 2 (1985).
15. S.-J. Hwu and J. D. Corbett, *J. Solid State Chem.* **64,** 331 (1986).
16. T. Hughbanks and J. D. Corbett, *Inorg. Chem.* **27,** 2022 (1988).

17. A. CISAR, Ph.D. Dissertation, Iowa State University, Ames, IA (1978).
18. H. IMOTO, J. D. CORBETT, AND A. CISAR, *Inorg. Chem.* **20,** 145 (1981).
19. A. SIMON, *Z. Anorg. Allg. Chem.* **355,** 311 (1967).
20. P.-J. CHU, R. P. ZIEBARTH, J. D. CORBETT, AND B. C. GERSTEIN, *J. Amer. Chem. Soc.* **110,** 5324 (1988).
21. A. CISAR, J. D. CORBETT, AND R. L. DAAKE, *Inorg. Chem.* **836 (1979).**
22. L. M. SEAVERSON AND J. D. CORBETT, *Inorg. Chem.* **22,** 2789 (1983).
23. S. D. WIJEYESEKERA AND J. D. CORBETT, unpublished research (1984).
24. R. P. ZIEBARTH AND J. D. CORBETT, to be submitted.
25. H. SCHÄFER, "Chemical Transport Reactions," Chap. 2, Academic Press, New York (1964).
26. S.-J. HWU, R. P. ZIEBARTH, S. V. WINBUSH, J. E. FORD, AND J. D. CORBETT, *Inorg. Chem.* **25,** 283 (1986).
27. J. ZHANG AND J. D. CORBETT, unpublished research.
28. R. P. ZIEBARTH AND J. D. CORBETT, *J. Amer. Chem. Soc.* **111,** in press (1989).
29. D. H. GUTHRIE AND J. D. CORBETT, *Inorg. Chem.* **21,** 3290 (1982).
30. S.-J. HWU, J. D. CORBETT, AND K. R. POEPPELMEIER, *J. Solid State Chem.* **57,** 43 (1985).
31. R. P. ZIEBARTH, J. ZHANG, AND J. D. CORBETT, unpublished research (1986).
32. G. ROSENTHAL AND J. D. CORBETT, *Inorg. Chem.* **27,** 53 (1988).